

## The sedimentology of river confluences

Sambrook-Smith, Greg; Dixon, Simon

DOI:

[10.1111/sed.12504](https://doi.org/10.1111/sed.12504)

License:

Creative Commons: Attribution (CC BY)

*Document Version*

Publisher's PDF, also known as Version of record

*Citation for published version (Harvard):*

Sambrook-Smith, G & Dixon, S 2019, 'The sedimentology of river confluences', *Sedimentology*, vol. 66, no. 2, pp. 391-407. <https://doi.org/10.1111/sed.12504>

[Link to publication on Research at Birmingham portal](#)

### General rights

Unless a licence is specified above, all rights (including copyright and moral rights) in this document are retained by the authors and/or the copyright holders. The express permission of the copyright holder must be obtained for any use of this material other than for purposes permitted by law.

- Users may freely distribute the URL that is used to identify this publication.
- Users may download and/or print one copy of the publication from the University of Birmingham research portal for the purpose of private study or non-commercial research.
- User may use extracts from the document in line with the concept of 'fair dealing' under the Copyright, Designs and Patents Act 1988 (?)
- Users may not further distribute the material nor use it for the purposes of commercial gain.

Where a licence is displayed above, please note the terms and conditions of the licence govern your use of this document.


When citing, please reference the published version.

### Take down policy

While the University of Birmingham exercises care and attention in making items available there are rare occasions when an item has been uploaded in error or has been deemed to be commercially or otherwise sensitive.

If you believe that this is the case for this document, please contact [UBIRA@lists.bham.ac.uk](mailto:UBIRA@lists.bham.ac.uk) providing details and we will remove access to the work immediately and investigate.

## The sedimentology of river confluences

GREGORY H. SAMBROOK SMITH\*, ANDREW P. NICHOLAS†, JAMES L. BEST‡ , JONATHAN M. BULL§, SIMON J. DIXON\*, STEVEN GOODBRED¶, MAMINUL H. SARKER\*\* and MARK E. VARDY§

\*School of Geography, Earth and Environmental Science, University of Birmingham, Birmingham B15 2TT, UK (E-mail: g.smith.4@bham.ac.uk)

†Geography, College of Life and Environmental Sciences, University of Exeter, Exeter EX4 4RJ, UK

‡Departments of Geology, Geography and Geographic Information Science, Mechanical Science and Engineering and Ven Te Chow Hydrosystems Laboratory, University of Illinois at Urbana-Champaign, Urbana, IL 61801, USA

§National Oceanography Centre Southampton, University of Southampton, Southampton SO14 3ZH, UK

¶Department of Earth and Environmental Sciences, Vanderbilt University, Nashville, TN 37240, USA

\*\*Centre for Environmental and Geographic Information Services, House 6, Road 23/C, Gulshan-1, Dhaka 1212, Bangladesh

Associate Editor – Charlie Bristow

### ABSTRACT

Channel confluences are key nodes within large river networks, and yet surprisingly little is known about their spatial and temporal evolution. Moreover, because confluences are associated with vertical scour that typically extends to several times the mean channel depth, the deposits associated with such scours should have a high preservation potential within the rock record. Paradoxically, such scours are rarely observed, and their preservation and sedimentological interpretation are poorly understood. The present study details results from a physically-based morphodynamic model that is applied to simulate the evolution and alluvial architecture of large river junctions. Boundary conditions within the model were defined to approximate the junction of the Ganges and Jamuna rivers, Bangladesh, with the model output being supplemented by geophysical datasets collected at this junction. The numerical simulations reveal several distinct styles of sedimentary fill that are related to the morphodynamic behaviour of bars, confluence scour downstream of braid bars, bend scour and major junction scour. Comparison with existing, largely qualitative, conceptual models reveals that none of these can be applied simply, although elements of each are evident in the deposits generated by the numerical simulation and observed in the geophysical data. The characteristics of the simulated scour deposits are found to vary according to the degree of reworking caused by channel migration, a factor not considered adequately in current conceptual models of confluence sedimentology. The alluvial architecture of major junction scours is thus characterized by the prevalence of erosion surfaces in conjunction with the thickest depositional sets. Confluence scour downstream of braid bar and bend scour sites may preserve some large individual sets, but these locations are typically characterized by lower average set thickness compared to major junction scour and by a lack of large-scale erosional surfaces. Areas of deposition not related to any of the specific scour types highlighted above record the thinnest depositional sets. This variety in the alluvial architecture of scours may go some way towards explaining the paradox of ancient junction

scours, that while abundant large scours are likely in the rock record, they have been reported rarely. The present results outline the likely range of confluence sedimentology and will serve as a new tool for recognizing and interpreting these deposits in the ancient fluvial record.

**Keywords** Alluvial architecture, confluence scour, large river, numerical model, preservation potential.

## INTRODUCTION

Deposits from rivers form an important part of the geological record, providing critical information about past Earth surface environments, as well as forming mineral resources, reservoirs for hydrocarbons, water and potential sites for CO<sub>2</sub> storage. The need for accurate fluvial depositional models that can quantify their geometry and heterogeneity is thus important in a variety of economic and societal contexts.

Despite their importance, there are a number of unresolved issues that concern how fluvial deposits are interpreted from the ancient sedimentary record. Channel confluences form ubiquitous components of all river networks (Best & Rhoads, 2008) and represent a sedimentary archive containing information on both the dynamics of these sites and, through the provenance of their sediments, the basins from which they are sourced (Goodbred *et al.*, 2014). Confluences adopt especial significance, in that it is often argued that the alluvial sedimentary record is biased towards preservation of sediments deposited in the deepest parts of channels (Paola & Borgman, 1991), such as confluence scours (Sambrook Smith *et al.*, 2005), which provide accommodation space that is less likely to be reworked during subsequent incision (Huber & Huggenberger, 2015). Confluences may thus be one of the sites of significant scour that set the deepest level, or ‘combing depth’ (*cf.* Paola & Borgman, 1991), to which a channel may erode and above which it deposits its sedimentary fill. However, while the importance of confluence scours as archives of fluvial deposits is universally acknowledged, there is no consensus as to what characterizes the fill of such scours. Current conceptual models are largely qualitative and often conflicting. For example, some research suggests that the fill of confluences will be broadly similar to the deposits of compound bars (Bridge, 2003; Bridge & Lunt, 2006), whilst others emphasise the presence of large cross-sets (Bristow *et al.*, 1993; Ullah *et al.*,

2015) or distinctive packages of erosional surfaces and associated fill (Siegenthaler & Huggenberger, 1993).

This lack of clarity as to what defines the fill of river confluences is, in large part, due to the considerable logistical problems encountered when attempting to measure the fill of active confluences in modern channels. Thus, most conceptual models are based on spatially and temporally limited observations, which may not fully capture the complexities of the processes of sedimentary fill. To overcome these shortcomings, the present paper uses a numerical model to simulate the morphodynamics of the confluence zone and investigate its associated sedimentology. These results provide high resolution information on the fill of channel confluences in order to: (i) evaluate a numerical model of confluence zone morphodynamics and associated alluvial architecture using seismic reflection and morphological data from one of the world’s largest river systems, the Jamuna (Brahmaputra) River, Bangladesh; (ii) quantify the prevalence of different sedimentary styles within the model output and assess to what extent these are linked to the river morphodynamics; and (iii) identify how the simulated scour deposits become modified over time.

## METHODS AND STUDY SITES

The morphodynamics and deposits of a large river confluence were simulated using a physically-based, two-dimensional, numerical model (HSTAR – Hydrodynamics and Sediment Transport in Alluvial Rivers) that represents water flow, sediment transport (for two size fractions; sand and silt), bank erosion and floodplain formation. The model has been described in detail and evaluated elsewhere (Nicholas *et al.*, 2013), and shown to be suitable for representing a range of large sand-bed rivers (Nicholas, 2013). In particular, unit bars, the key building block of sand-bed rivers, are an emergent

characteristic of the simulations, resulting directly from patterns of modelled erosion and deposition, although it should be noted that smaller-scale bedforms (for example, dunes and ripples) are not resolved within the model. The HSTAR model solves the two-dimensional, depth-averaged, shallow water equations written in conservative form. Model equations are solved on a structured grid (resolution  $\Delta x$ ,  $\Delta y$ ) within which each grid cell is defined as either active river bed or floodplain (including vegetated islands). For active river bed cells, total sand transport (bedload and suspended load) is modelled using the Engelund–Hansen (1967) transport law. For hydraulic roughness, a constant Chezy value of  $50 \text{ m}^{0.5} \text{ s}^{-1}$  is used in all channels and  $15 \text{ m}^{0.5} \text{ s}^{-1}$  on vegetated surfaces. The model domain (Fig. 1) was set-up to be broadly comparable to the confluence of the Jamuna and Ganges rivers in Bangladesh (see Best & Ashworth, 1997; Fig. 2), for which associated high-resolution seismic reflection surveys,

and analysis of planform evolution, was undertaken. All simulations were conducted using a model domain 66 km long ( $x$  direction) by 48 km wide ( $y$  direction). This resulted in a model with  $1100 \times 800$  cells, each measuring 60 m long by 60 m wide. The initial width of the two simulated channels upstream of the confluence was 3.6 km and 1.8 km, respectively, with initial channel width downstream of the confluence being *ca* 4 km. The planform configuration of the model was also similar to the field site, with the channel downstream of the confluence forming a  $27^\circ$  angle to the axis of the major incoming channel. Bank erosion rates are modelled as the product of the bank gradient, the total rate of sediment transport parallel to the bankline, and a dimensionless bank erodibility constant. To capture the planform change observed in the field (Fig. 2), the bank erodibility constant was set to be lower (i.e. stronger banks) for the smaller upstream tributary channel and the channel downstream of the

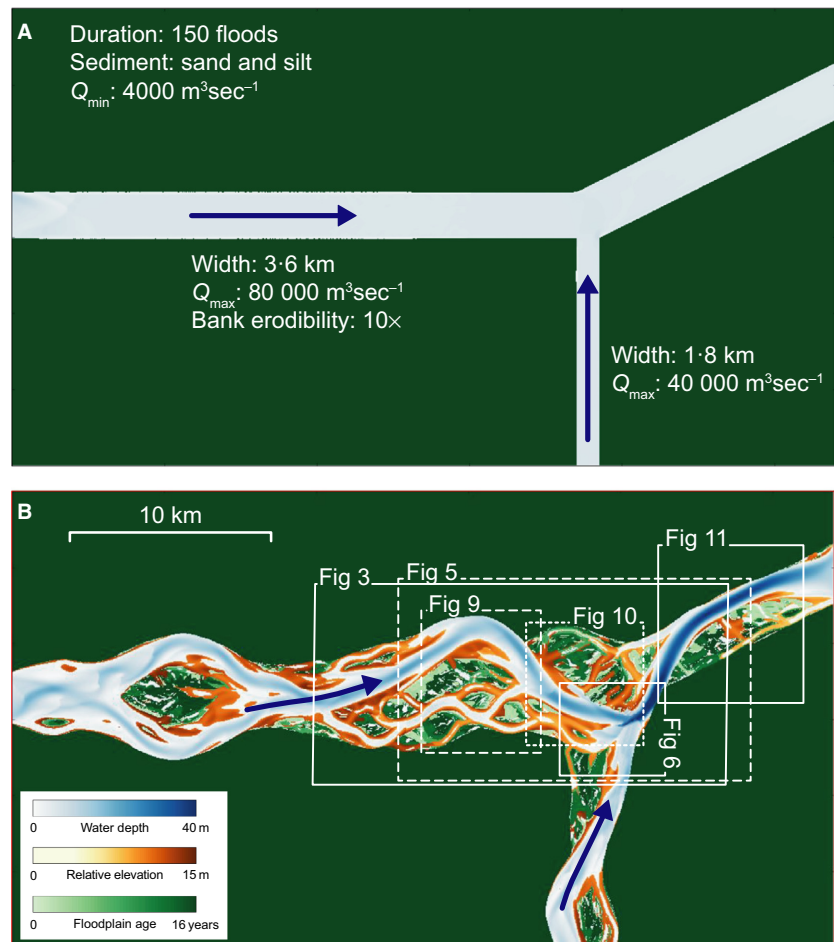


**Fig. 1.** (A) Initial numerical model configuration and boundary conditions. (B) Modelled planform at the end of the simulation with locations of other figures referred to in the text.

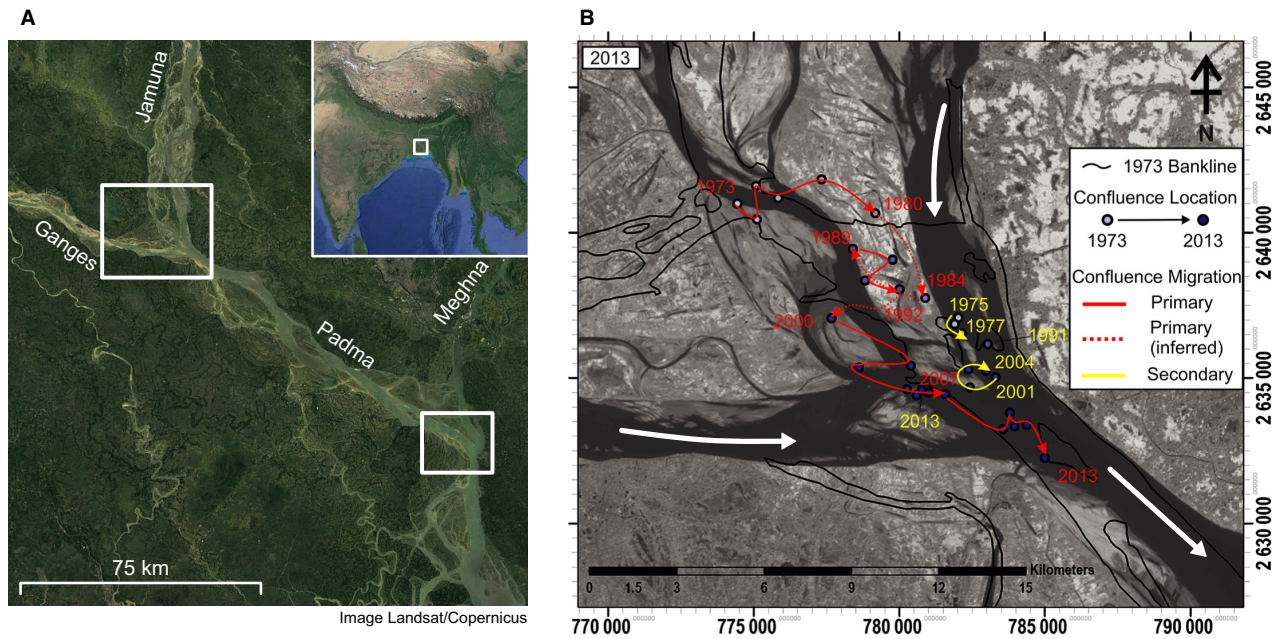


**Fig. 2.** (A) Image of the field sites in Bangladesh illustrating the location of Jamuna–Ganges (upstream) and Padma–Meghna (downstream) confluences. (B) Diagram illustrating the dynamic nature of the Jamuna–Ganges confluence. Background image is from 2013, with black lines showing the banklines from 1973. Each coloured dot represents a single confluence location as inferred from annual low flow imagery (Landsat, 30 m pixel resolution). The colour ramp for the dots representing confluence location goes from dark blue for the earliest (1973), through to light blue, for the most recent (2013). Dotted lines are pathways along which it is inferred that the confluence has migrated, solid lines are paths where it is known that the confluence has migrated due to a better temporal sequence of imagery with no missing years. In some years, it is interpreted that there would probably have been a bifurcated junction with a smaller confluence in addition to the primary junction indicated by the coloured dots highlighted above. These latter sites are shown as yellow years and arrows on the figure.

confluence, but higher (i.e. weaker banks) for the larger incoming tributary. Finally, the simulated flow regime was also broadly similar to the field site, with low flow and peak discharges for the larger channel of  $4000 \text{ m}^3 \text{ s}^{-1}$  and  $80\,000 \text{ m}^3 \text{ s}^{-1}$ , respectively, to reflect the monsoon-dominated regime. Flows in the smaller channel were 50% of that in the main channel. Simulated inflow conditions consisted of a series of regular symmetrical hydrographs, where discharge ( $Q$ ) as a function of time is:

$$Q = Q_{\text{low}} + (Q_{\text{max}} - Q_{\text{low}})((1 + \sin(2\pi T - \pi/2))/2)^{3.5}$$

where  $T$  is time normalised by the hydrograph duration (i.e.  $T$  increases from 0 to 1 over the course of the hydrograph),  $Q_{\text{low}}$  is the low flow discharge, and  $Q_{\text{max}}$  is the flood peak discharge. It should be noted that the aim of the modelling reported herein is to investigate the confluence dynamics and associated deposits of rivers with similar general characteristics to those of the

study site, rather than to reproduce the specific channel behaviour observed at the Jamuna–Ganges confluence.

Simulations ran for a sequence of 150 annual flood hydrographs, therefore allowing considerable morphodynamic evolution (Fig. 3) and significant reworking of deposits to occur. The model was used to generate pseudo-sections of preserved stratigraphy, from the erosional and depositional surfaces derived from the modelled topography, which were compared to seismic data collected from the field. Erosional and depositional surfaces are simply defined as topographic surfaces joining locations that underwent erosion and deposition respectively in the previous model time step. Surfaces were extracted eight times per flood event, and thus the modelled stratigraphy shown herein is based on 1200 points in time. These surfaces were then used to generate metrics (defined in Fig. 4) derived from pseudo-sections (two-dimensional slices) through the modelled stratigraphy to



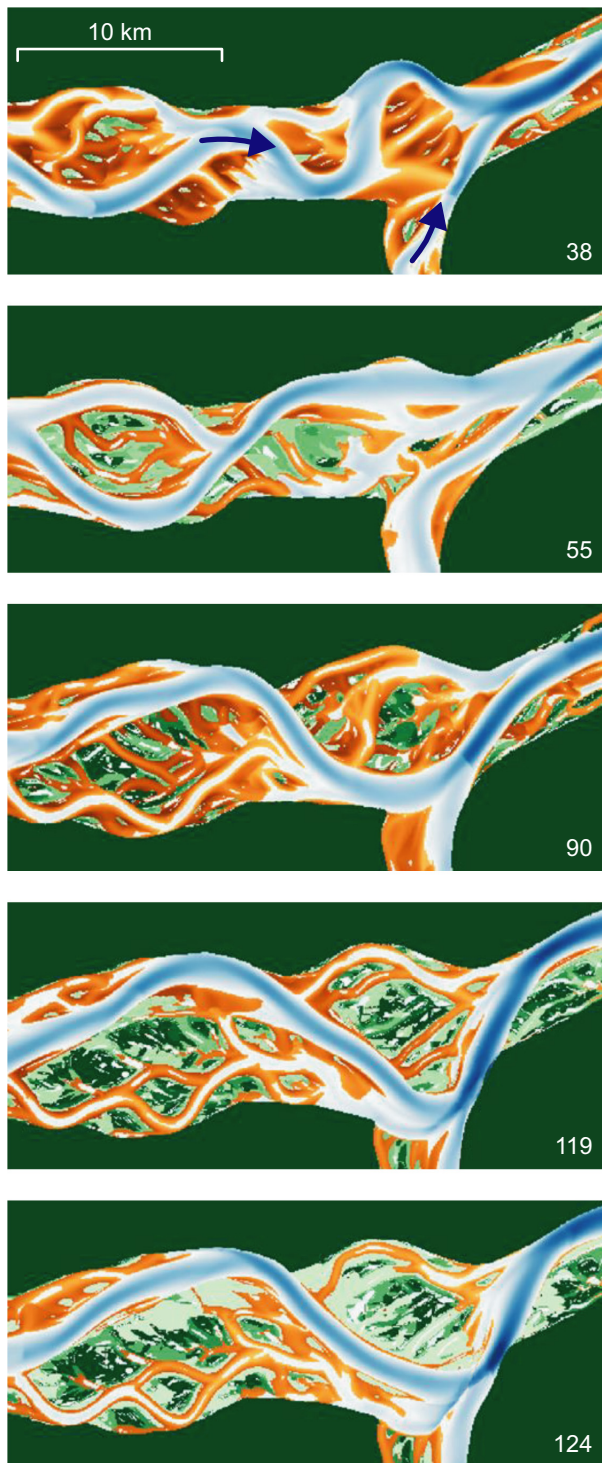


**Fig. 3.** Evolution of the confluence planform extracted for different floods in the sequence of modelled results. Location of images within the model domain and legend are shown in Fig. 1. See text for further discussion.

establish the characteristics of the sedimentology. To achieve this, packages of preserved sediment, defined as discrete units of sediment

completely bounded by topographic surfaces, were identified. Two metrics were then calculated (see Fig. 4) for each package: (i) the vertical extent of each package ( $V_x$ ) which is equal to the maximum minus the minimum elevation of any bounding surface for the package; and (ii) the lateral extent of each package ( $L_x$ ) which is equal to the horizontal distance from the left to the right-hand limit of the package. Metrics were calculated for discrete portions of the simulated deposits, representing the sedimentary fill of contrasting scours. This comprised 40 cross-sections for each type, except the bar deposits associated with no scour where only 20 cross-sections were used given the smaller area of deposits. The number of sediment packages within each fill, and at each channel section, varied over the course of the simulation as sediment was deposited and reworked. Herein, the pdf (probability density function) of the package metrics is characterized using the 10th, 50th and 90th percentiles of the distribution. In addition to the metrics  $L_x$  and  $V_x$ , the thickness of alluvial sets (setH) was also calculated (see Fig. 4), where set boundaries were defined by their erosion surfaces and using the methodology of van de Lageweg *et al.* (2016). Set thickness calculations were conducted for each model grid cell across a cross-section, rather than for sediment packages, because the latter are bounded by both erosional and depositional surfaces (see Fig. 4). The pdf of set thickness values for each sedimentary fill at each channel cross-section was used to determine the 10th, 50th and 90th percentiles of setH values.

The planform evolution of the model simulation was compared to the Jamuna–Ganges confluence site using georeferenced Landsat imagery spanning the period 1972 to 2014, which was analysed to quantify the migration of this junction (Dixon *et al.*, 2018). To provide comparison between the simulated model deposits and the Jamuna–Ganges confluence, seismic reflection profiles were acquired in June 2014 from a survey boat, using a Boomer system consisting of an Applied Acoustics AA200 plate (Applied Acoustics Engineering Limited, Great Yarmouth, UK) mounted on a small, lightweight catamaran, with data recorded using a single-channel mini-streamer. The raw trace data were combined with DGPS positional information obtained using a Hemisphere R131 with OmniSTAR correction data (OmniSTAR, Leidschendam, The Netherlands), and processed using standard seismic processing software to

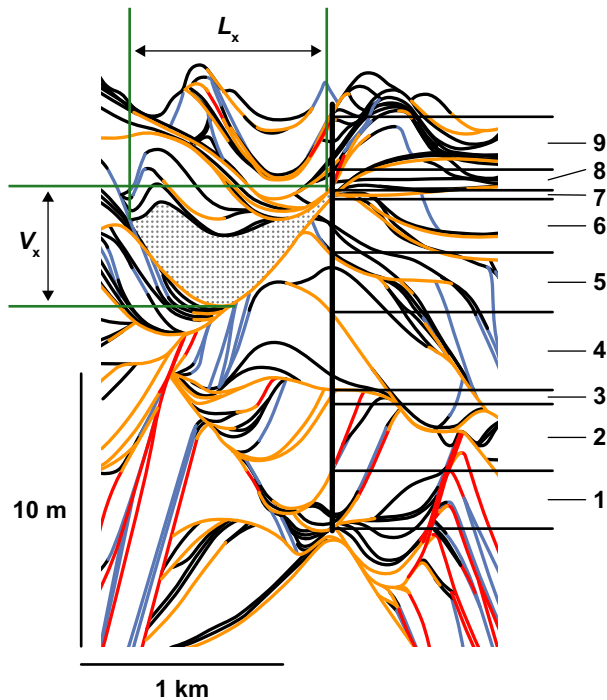


**Fig. 4.** Pseudo-section of a bar that has evolved away from any significant scour topography. Figure 11 shows the context of where this bar is located. Blue and black lines are  $>1^\circ$  and  $<1^\circ$  angle depositional surfaces, respectively, red and yellow lines are  $>1^\circ$  and  $<1^\circ$  angle erosional surfaces, respectively. Also illustrated is an example of how  $L_x$  and  $V_x$  of a sedimentary package are defined, as well as set thickness (setH). For illustration, the solid vertical black line indicates a virtual core with nine sets that comprise the compound bar in the simulation (yellow/red surfaces represent episodes of erosion that define the set boundaries).

minimise noise contamination and optimize signal coherence and interpretability. While the main field study site discussed herein is the Jamuna–Ganges confluence, some additional seismic data were also collected downstream at the junction of the Padma and Meghna rivers (Fig. 2).

## RESULTS

### Confluence morphodynamics

The model results reveal that the principal junction scour is not static over the duration of the simulation, but instead displays a broad range of behaviours (Fig. 3). Moreover, the area of the confluence scour can be extensive with respect

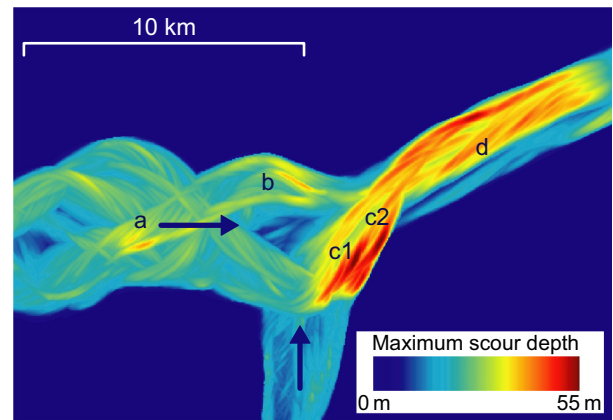


**Fig. 5.** Basal erosion surface at the end of the model simulation, with the four types of scour discussed in this paper indicated as: a = bar-scale confluence; b = bend scour; c = confluence scour (locations 1 and 2 show scour migration); and d = downstream of confluence. Location of image within the model domain is shown in Fig. 1.

to the channel width. For example, the junction scour can extend from downstream of where the two channels meet and back into the tributaries (flood 38; Fig. 3), to cases where the scour is less distinct and more restricted in its spatial extent (flood 55; Fig. 3). The two tributary channels display contrasting planform morphologies, most notably with the main tributary having a dominance of either its left or right anabranch channel at the confluence (compare floods 55 and 90, Fig. 3). Similarly, the smaller tributary can approach the junction on either its left or right side depending on the location of the bank-attached bar that forms at the downstream end of this channel (compare floods 55 and 90, Fig. 3). After flood 90, the broad configuration of the confluence zone does not change significantly, although the main scour is still migratory, as illustrated by the downstream movement of the deepest scour between floods 119 and 124 (Fig. 3). The overall spatial extent of scour associated with the confluence zone is best illustrated by reference to the basal erosion surface at the end of the simulation (Fig. 5). This plot shows that scour upstream of the confluence is either very modest (in the case of the smaller tributary) or very restricted in spatial extent, such as the bar-scale confluence and bend scour seen in the main tributary (labelled 'a' and 'b', respectively, in Fig. 5). Conversely, where the two tributaries meet, and for a significant distance downstream, the bed is

characterized by an extensive, continuous deep scour that is very different in character (Fig. 5).

Based on analysis of the Landsat imagery, the Jamuna–Ganges confluence has shown appreciable migration and has not been fixed in its planform position (Best & Ashworth, 1997; Dixon *et al.*, 2018). Overall, since 1973, the confluence has migrated *ca* 12 km south-east (Fig. 2B), although there is a great deal of variability in both the magnitude and direction of confluence migration over the period 1972 to 2014. Annual migration rates range from a few hundred metres up to almost 2 km. Migration of the confluence has generally been to the south-east (i.e. downstream), but between 1984 and 1989 the junction moved *ca* 4 km upstream (Fig. 2B). The planform behaviour of the tributaries at the field site was also variable, as observed in the model output. For example, in 1973 (see background image, Fig. 2B) the east side of the Jamuna River was the larger

anabranch, but the western channel has adopted dominance in previous time periods. The imagery of the Jamuna–Ganges confluence thus confirms, at least from a qualitative perspective, the broad range of behaviours described from the model output.

### Confluence sedimentology

Before presenting the model results, it is useful to consider what the simulated pseudo-sections might relate to in terms of the rock record. The composite basal surface seen in the model results (for example, Fig. 6) is comparable to the scale of a sixth-order channel belt basal surface (*sensu* Miall, 1985). The smallest scale of morphological feature simulated within the model is a unit bar, and thus surfaces related to dunes and ripples are not present in the model results (i.e. second-order surfaces and below). In terms

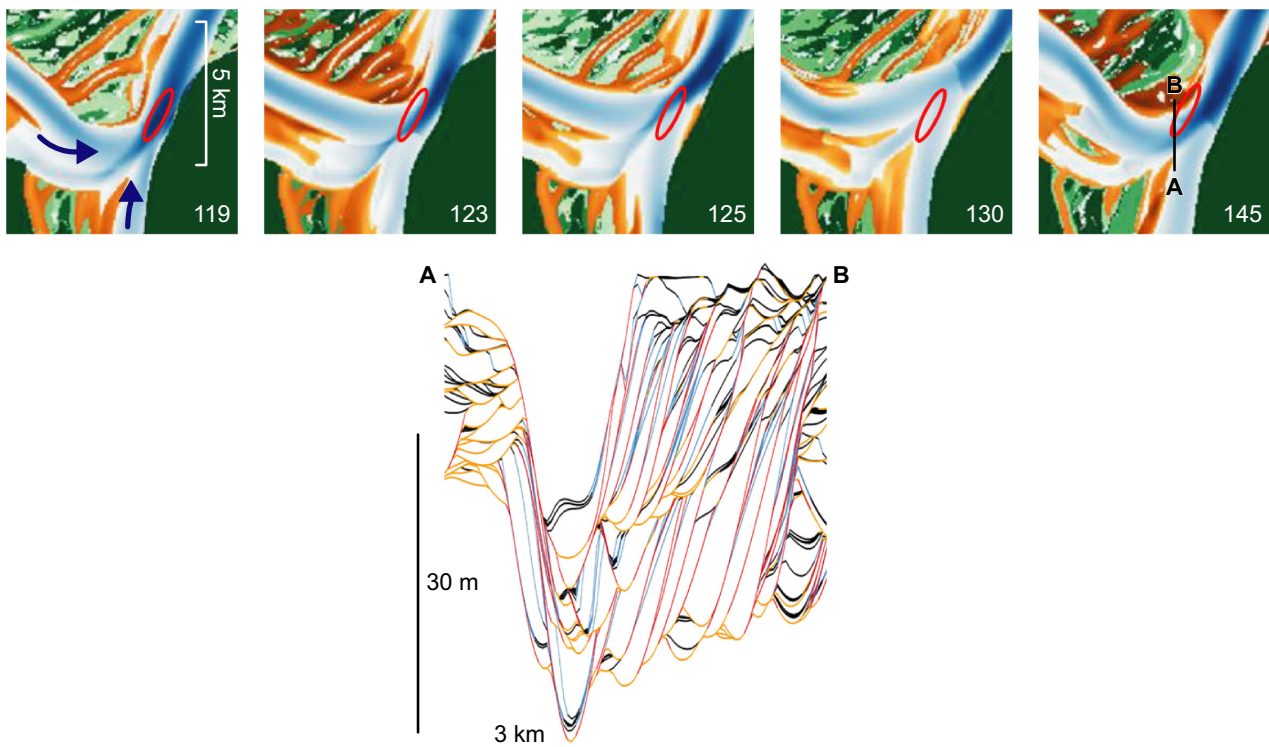


**Fig. 6.** Time series of confluence planform showing how the scour migrates downstream and is filled with tributary mouth bars from both upstream channels, which are then overlain by lateral accretion deposits generated by an expanding point bar (location of images within the model domain and legend are shown in Fig. 1). Also shown is an associated pseudo-section (location shown on planform map of time-step 145), with blue and black lines depicting  $>1^\circ$  and  $<1^\circ$  angle depositional surfaces, respectively, and red and yellow lines are  $>1^\circ$  and  $<1^\circ$  angle erosional surfaces, respectively. In the lower part of the pseudo-section, channel-scale depositional surfaces (blue) formed by the migrating tributary mouth bars are clearly seen, with evidence of migration from either direction in the lower part of the profile. Also seen are parallel erosion surfaces (red) indicating migration of the scour as the point bar has expanded.



of scale, the pseudo-sections are thus comparable with third to sixth-order bounding surfaces in the rock record. However, it is important to reiterate that these are pseudo-sections, and a direct like-for-like comparison between model and field is not possible currently.

Some sections of the modelled sedimentology show a dominance of large (defined here as equivalent to the channel depth), depositional surfaces (blue lines in Fig. 6; angle up to  $4^\circ$ ) that, based on the evolution in planform morphology, are produced by tributary mouth bars migrating into the confluence. This depositional characteristic is also shown by field evidence from the Padma–Meghna junction (Fig. 7) where tributary mouth bars have migrated towards a *ca* 50 m deep scour and result in clear, dipping (*ca*  $3^\circ$ ), high-amplitude seismic reflection surfaces (*ca* 15 m in height) that represent the successive locations of the migrating bar margin.

In contrast to these depositional surfaces, the model output can also be dominated by erosional surfaces. Comparison with the planform model morphodynamic data shows that the

migration of the simulated scour in a broadly downstream and left to right direction (see Figs 5 and 6) is manifested in the deposits by generation of sequential large erosion surfaces (red lines in Fig. 6; angle up to  $2^\circ$ ). This depositional characteristic is also seen in the seismic reflection profiles collected at the Jamuna–Ganges confluence (Fig. 8A), which shows three reflections (R1 to R3) on the east side, that are parallel with the current bed surface (i.e. *ca*  $1^\circ$ ) at successively greater depths down to *ca* 14 m, and which can be traced over distances of up to 1 to 2 km. These reflections are interpreted as erosional surfaces that record the east to west lateral movement of the scour.

In contrast to those areas where there are strong depositional or erosional signatures, many sections of the model output show a more complex combination of very low-angle ( $<1^\circ$ ) erosional and depositional surfaces that are heterogeneous in nature. In these sections, cross-cutting surfaces and deposits are often prevalent as compared with the sequential,

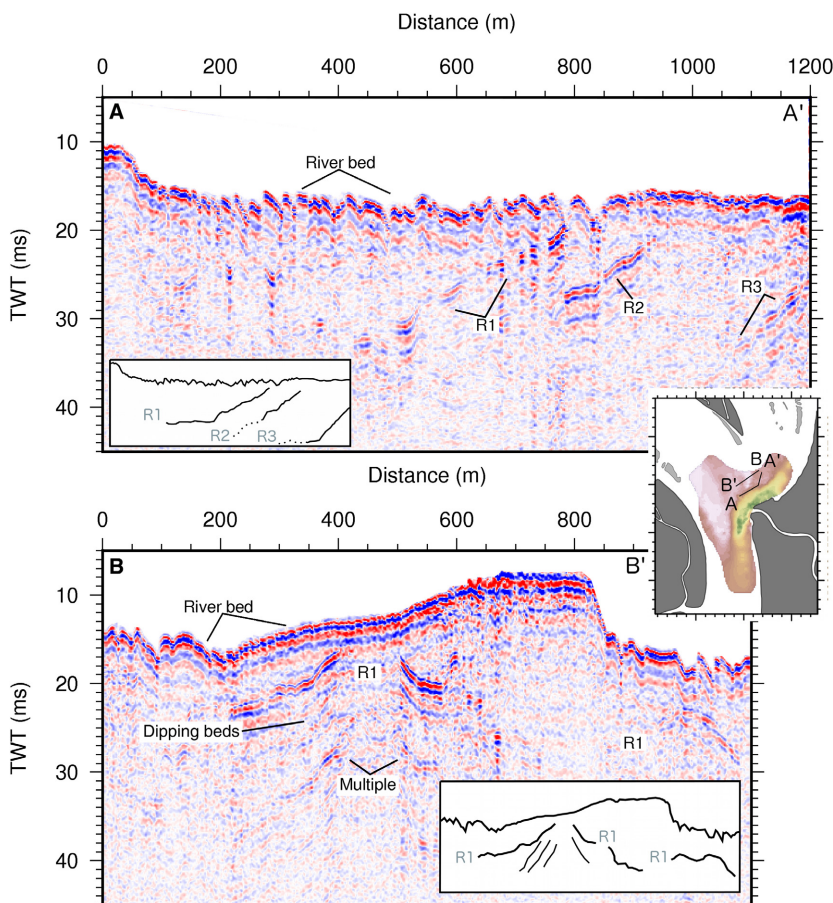
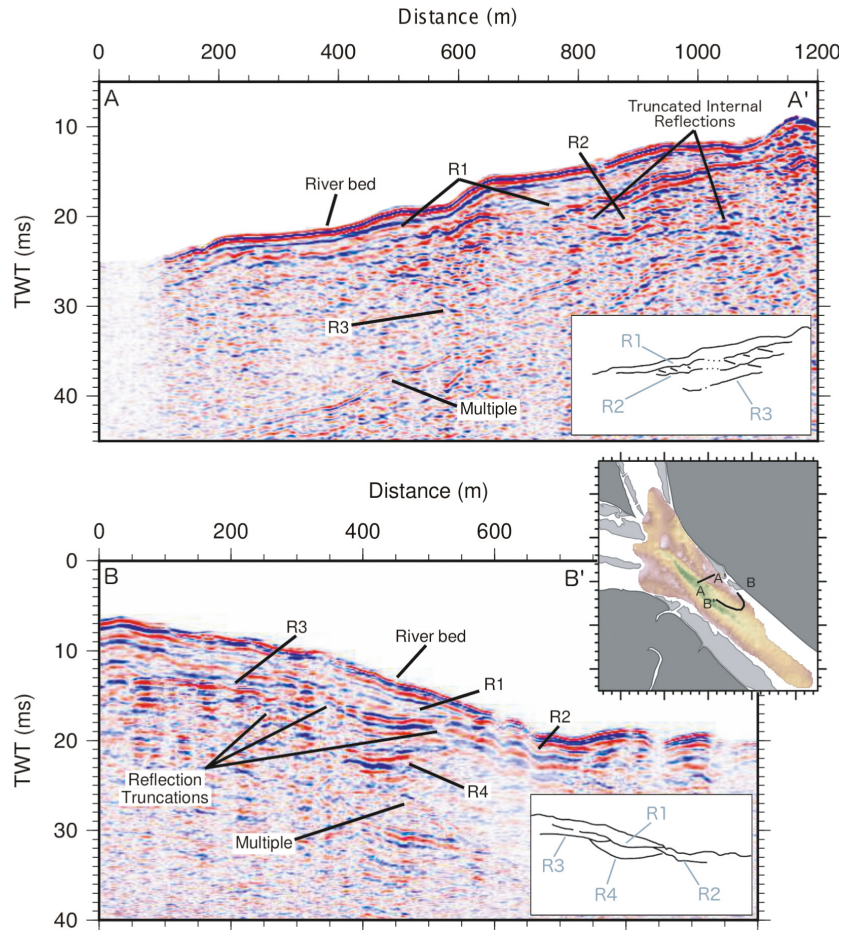


**Fig. 7.** Seismic data and interpretations from the Padma–Meghna junction (see Fig. 2A for location). Inset shows bathymetry and location of seismic lines at the site. Reflections R1, R2 and R3 are interpreted as large sets (up to *ca* 15 m in height) associated with the downstream and lateral growth of a bar as it has migrated towards the scour.

**Fig. 8.** (A) Seismic data and interpretations from the Jamuna–Ganges junction (see Fig. 2A for location). Inset shows bathymetry and location of seismic line at the site. Note the three broadly parallel reflections, labelled R1 to R3, interpreted herein as erosion surfaces that can be traced within the data on the east side of the confluence. (B) Seismic data and interpretations from the Jamuna–Ganges junction (see Fig. 2A for location). Inset shows bathymetry and location of seismic line at the site. The data shows a series of relatively short cross-cutting reflections (R1 to R4) that are indicative of migration and reworking of sediment by the scour zone. Note that reflections R1 to R3 refer to the same feature in both parts of the figure.



parallel, surfaces described previously. This observation is also demonstrated in the data concerning the typical dimensions of deposits in the simulated pseudo-sections (Table 1). Modelled depositional packages are predominantly <1 km long, and much smaller than the scale of the channel width or bar length, as are the majority of reflections in the seismic data. For example, the seismic reflections seen at the channel margin (Fig. 8A) have a more complicated spatial arrangement when seen at the base of the scour at the Jamuna–Ganges confluence (Fig. 8B). Here the reflections show clear truncations, and are typically only *ca* 400 m in length. These relationships, in both model and field, are indicative of channel movement with no preferred orientation, and are likely to be the product of the thalweg migrating back across a location and thus reworking its deposits.

The results presented above indicate that, from a qualitative perspective, the model is producing successfully the basic morphodynamic and sedimentological characteristics of the large

confluences in Bangladesh. Due to the scale of the field channels, it was not possible to survey comprehensively the entire area of the Jamuna–Ganges confluence to quantify any potential spatial patterns in the surfaces described above. This is, however, possible for the model results. Based on Fig. 5, four different components of scour can be recognized that are associated with: (i) a confluence at the downstream end of a braid bar (labelled ‘a’ in Fig. 5); (ii) channel deepening on the outside of a bend (labelled ‘b’ in Fig. 5); (iii) the principal confluence scour as the two tributaries meet (labelled ‘c’ in Fig. 5); and (iv) the extensive scour zone downstream of where the two channels meet (labelled ‘d’ in Fig. 5). The metrics of fill associated with these four zones are considered below, in order to examine whether the different scours have any defining characteristics. For further comparison, the fill associated with a non-scour (compound bar) site is also considered below, to examine the extent to which scour zones (of any type) may be differentiated from other deposits. The

	Bar confluence (m)	Bend scour (m)	Channel confluence (m)	Downstream of confluence (m)	Bar – No scour (m)
setH <sub>10</sub>	0.24	0.24	0.42	0.29	0.25
setH <sub>50</sub>	1.3	1.4	2.9	2.0	1.1
setH <sub>90</sub>	7.1	4.9	9.2	6.1	3.9
V <sub>x10</sub>	0.7	0.8	1.4	1.0	0.6
V <sub>x50</sub>	2.7	3.3	5.2	4.0	2.2
V <sub>x90</sub>	8.0	11.9	17.8	14.3	6.3
L <sub>x10</sub>	121	121	121	120	121
L <sub>x50</sub>	242	238	299	180	220
L <sub>x90</sub>	599	568	851	596	583
Depth <sub>max</sub>	32	32	48	44	15

Subscripts 10, 50 and 90 refer to the values for the 10th, 50th and 90th percentile of each parameter. Depth<sub>max</sub> is the maximum depth of scour recorded during the simulation for each location.

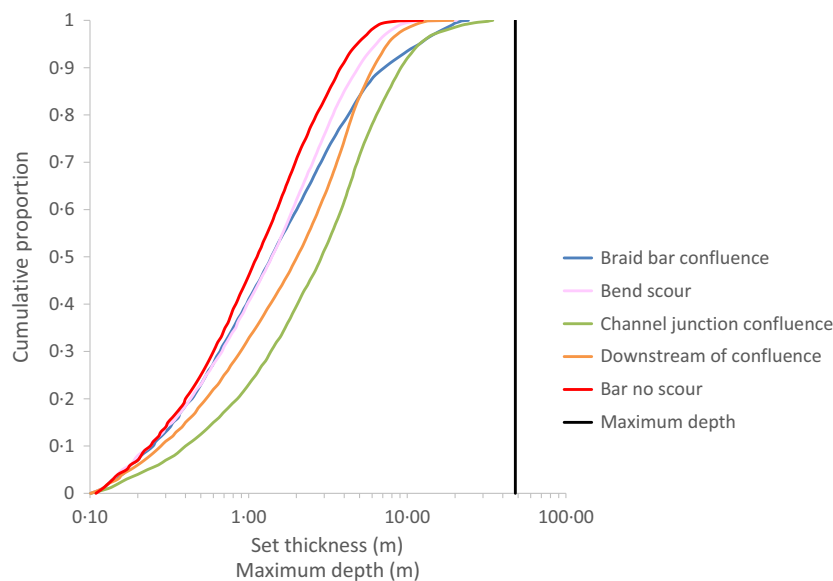


**Table 1.** Metrics extracted from the numerical model at the end of the simulation. SetH, V<sub>x</sub> and L<sub>x</sub> refer to set thickness, and deposit package vertical and lateral extent, respectively.

**Fig. 9.** Cumulative proportion distributions for set thickness (setH) within the four different scour locations and a braid bar that developed in an area of no scour. Also indicated is the likely maximum flow depth within the model domain, identified here as the distance between the maximum depth of the scour and the banktop elevation at the channel confluence location.

metrics of set thicknesses (Fig. 9), together with the vertical and lateral extent of depositional packages within the different scours and the bar, are given in Table 1. Below, each of the scour types within the model is described in turn.

#### *Scour associated with a braid bar confluence*

The original confluence scour is filled with unit bar sets that accrete laterally onto an expanding point bar (Fig. 10). As the main channel thalweg switches to the opposite side of the braidplain, a compound bar from upstream grows and enlarges to dominate the reach, and thus the original scour is preserved beneath, but with some reworking of the surface (Fig. 10). As a

result of reworking, the deposit metrics (Table 1, Fig. 9) indicate a relatively small median set thickness (1.3 m) with *ca* 11 sets in the centre of the fill, somewhat greater than the typical value of three to seven sets suggested by Bridge & Lunt (2006). However, as illustrated in Fig. 10, the lowermost sets are much thicker than the others, which is reflected in the relatively high 90th percentile value of set thickness (7.1 m) for this site. The vertical and lateral extent of sedimentary packages is, however, no different to the other sites, thus suggesting a high degree of truncation and reworking despite some thick sets being preserved. This observation is similar to that of radar data from compound bars in



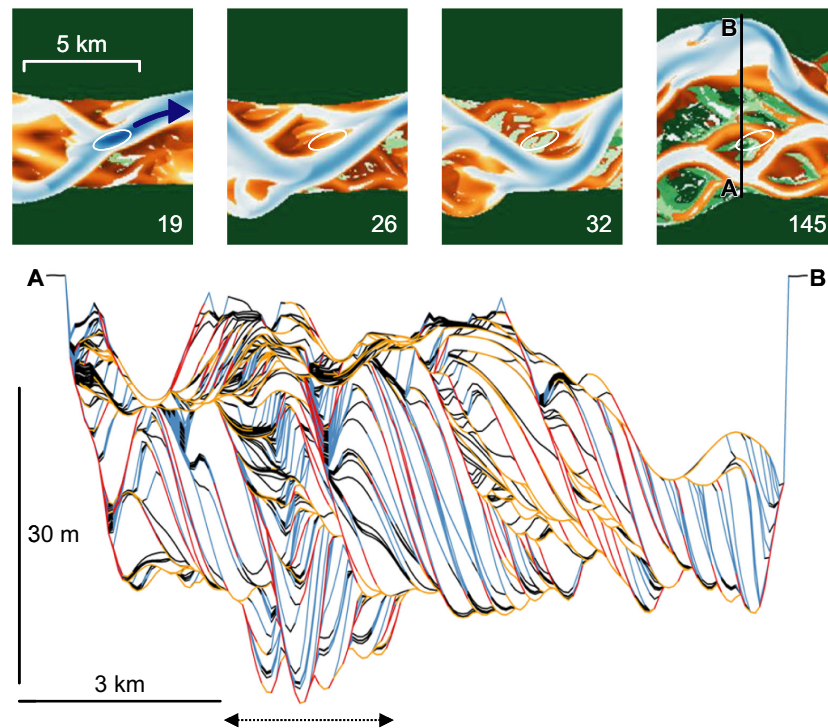


**Fig. 10.** Evolution of a braid bar confluence scour. Location of images within the model domain and legend is shown in Fig. 1. Scour forms downstream of a central bar in flood 19, with a bank-attached bar then expanding across the scour by lateral accretion of unit bars in floods 26 to 32. A large central bar then grows to dominate the reach, with the main channel switching to the other side and thus preserving the scour-fill structure within a large compound bar by the end of the simulation. A pseudo-section (see planform time-step 145 for location) taken through the upstream part of the original scour is also shown, with the dashed arrowed line indicating the spatial extent of the scour within the section. Blue and black lines are  $>1^\circ$  and  $<1^\circ$  angle depositional surfaces, respectively, whilst red and yellow lines are  $>1^\circ$  and  $<1^\circ$  angle erosional surfaces, respectively. A vertical profile through the pseudo-section indicates *ca* 11 sets, with noticeably thicker sets at the base.

large braided rivers, such as reported by Reesink *et al.* (2014) who noted that *ca* 10% of deposits from the Paraná River, Argentina, may be large depositional sets associated with unit bar slipfaces.

#### *Outer bend scour*

The evolution of the bend scour and associated sedimentology (Fig. 11) shows that this scour forms around flood 38, and is relatively fixed in its position, until changes to the upstream channel configuration result in a much lower sinuosity channel replacing the original meandering thalweg. As a result, channel depth decreases significantly and a scour is no longer present after flood 50. Instead, as the simulation progresses, the site becomes the focus for the emergence of a large point bar, with the original channel on the left bank gradually filling over time. These evolutionary trends result in deposit metrics that are very similar to those of the braid

bar confluence scour described above, although with one notable exception (Table 1, Fig. 9) in that the bend scour has a much lower 90th percentile value for set thickness. This is evident by comparison of Figs 10 and 11, and can be attributed to the more passive, non-migratory, style of fill at the bend scour. Thus, instead of the scour migrating relatively large distances and being filled by multiple migratory unit bars, the scour has remained relatively fixed, so that the accommodation space needed to generate more laterally extensive, and vertically variable, thick sets has not been created.

#### *Channel confluence scour*

The morphodynamic evolution of the main junction scour zone was discussed above (Figs 3 and 6). This deep scour migrated downstream, and towards the right bank, as it was successively filled by bars from both tributaries. The key feature of this fill is that for all of the



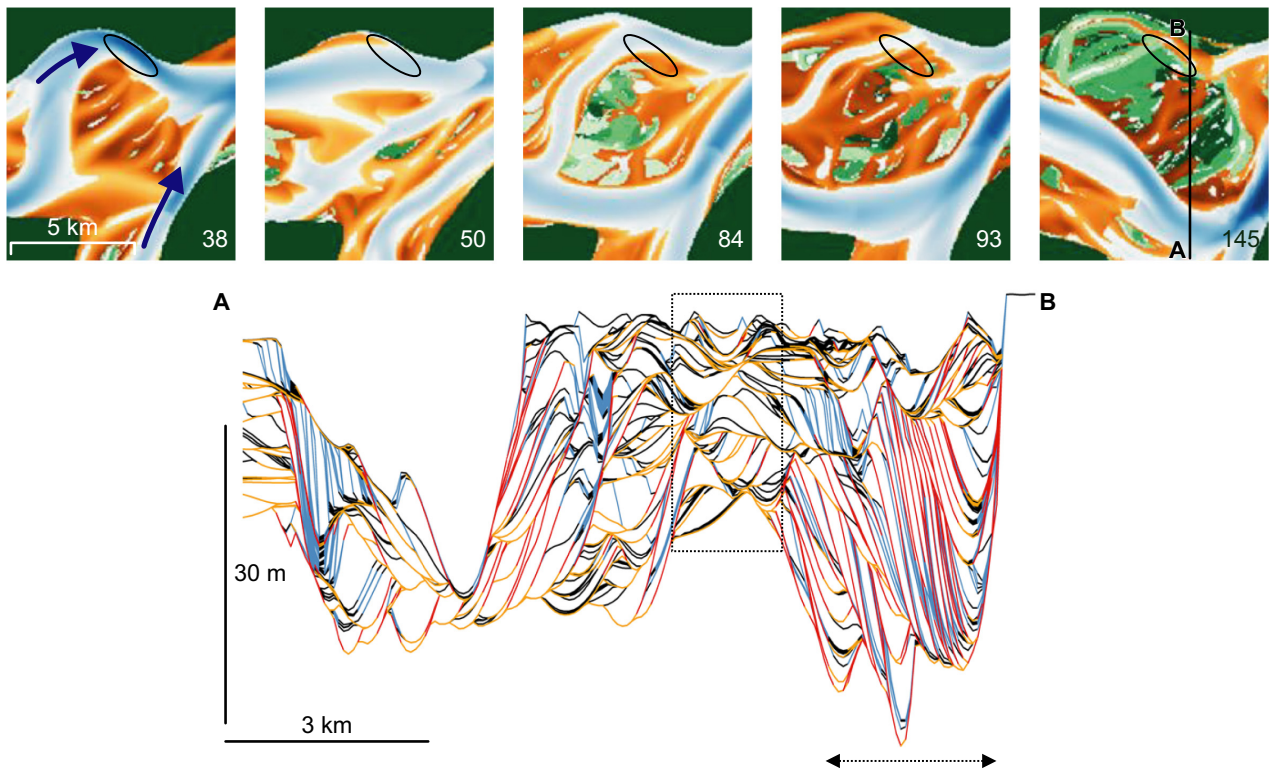


**Fig. 11.** Evolution of bend scour. Location of images within the model domain and legend are shown in Fig. 1. Scour forms on outer bend in flood 38, and between floods 43 to 61 the scour becomes shallower as a straighter thalweg moves across the original scour site. From flood 84 onwards, a large point bar becomes established at the site as the original channel gradually fills. The pseudo-section (location shown in plan map 145) displays the associated sedimentology. Blue and black lines are  $>1^\circ$  and  $<1^\circ$  angle depositional surfaces, respectively, whilst red and yellow lines are  $>1^\circ$  and  $<1^\circ$  angle erosional surfaces, respectively. The dashed arrowed line indicates the section of the fill associated with the bend scour, whilst the dashed box shows the location of the section presented in Fig. 4.

sedimentological metrics, this area records the largest values. Thus median set thickness (2.9 m) is double that of the bar-scale confluence and bend scour sites (Table 1, Fig. 9), and the thickest sets are also preserved here (for example, set thickness 90th percentile = 9.2 m). The deep scour, and resultant accommodation space that is filled, is also shown by high values of the vertical extent of packages, with the 50th and 90th percentiles being 5.2 m and 17.8 m, respectively (Table 1). The lateral extent of packages is, however, still relatively modest given the scale of the channel, with the 50th and 90th percentiles being 299 m and 851 m, respectively (Table 1).

#### *Downstream confluence zone*

The elongate scour zone that extends downstream from where the two channels join, displays a relatively stable planform morphology

over the simulation period when compared with the other scour sites described above. The deep thalweg thus migrates between the left bank and centre of the channel, while the right bank always possesses an attached bar (Fig. 12). Because the flow is always confined to one channel, flow depths remain deep throughout the simulation. In terms of the associated sedimentology, the sediments of the attached bar on the right bank remain largely pristine, and thus thick sets are preserved. However, in the rest of the channel, migration of the thalweg removes much of the previous sediment and also replaces this with fill of a similar type (i.e. channel-scale lateral accretion related to compound bar growth). As a result, despite this repeated reworking, large sets are prevalent in the metrics at this site (Table 1, Fig. 9), which in terms of magnitude show values between the channel confluence and the two upstream scours. For

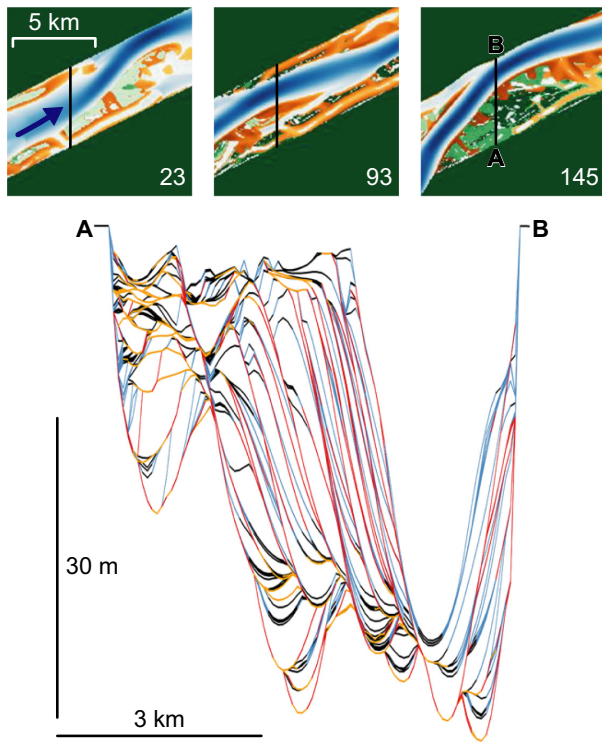


**Fig. 12.** Evolution of scour downstream of the confluence zone. Location of images within the model domain and legend are shown in Fig. 1. The morphodynamics show that the channel thalweg moves across a relatively narrow zone, in this example, from the centre (flood 23) to near the left bank (flood 93) and then against the left bank (flood 145), whilst a bar on the right bank is permanent throughout the simulation. An associated pseudo-section (see associated plan maps for location) is also shown. Blue and black lines are  $>1^\circ$  and  $<1^\circ$  angle depositional surfaces, respectively, whilst red and yellow lines are  $>1^\circ$  and  $<1^\circ$  angle erosional surfaces, respectively.

example, the 50th and 90th percentiles for set thickness are 2.0 m and 6.1 m, respectively. The low value of the median lateral extent of sediment packages probably reflects the high level of reworking discussed above.

#### *Bar deposits not associated with scour*

In order to compare the different types of scour that have been discussed above with non-scour sites, a section of simulated sedimentology associated with the deposits of a compound bar was analysed. Figure 11 provides the broad context of the bar evolution, whilst Fig. 4 shows an enlarged section through this compound bar. This vertical section (Fig. 4) demonstrates that the bar comprises nine sets, which is slightly greater than typical for a braid bar according to

the work of Bridge & Lunt (2006). Overall, due to the lack of scour, which negates the formation of large sets, and repeated sediment reworking, this site has the lowest values of set and sediment package dimensions (Table 1, Fig. 9). Thus, median set thickness is only 1.1 m and the 90th percentile is just 3.9 m. A similar pattern is seen for the vertical extent of packages (50th percentile = 2.2 m; 90th percentile = 6.3 m), although it should be noted that the lateral extent of packages is similar to the other scour sites, with the exception of the much larger channel confluence scour.

#### *Morphodynamics, reworking and preservation over time*

The elevation of the basal erosion surface for each of the sites discussed above shows a clear relationship between scour depth and set thickness (Table 1). Thus, deeper scours create the potential for larger sets to be deposited, as has been noted by others (Gardner & Ashmore, 2011). This tendency is similar to the control by dune trough depth on associated set thickness. The characteristics of the sets that are preserved within the scours after repeated episodes of reworking display a range of behaviours (Fig. 13) that relate to the mobility of the different scour zones. At the braid bar confluence (Fig. 14A), median set thickness is highly variable because the site is active (i.e. up to about flood 80); set thickness thus responds to the complex interactions of new bar growth and erosion, in conjunction with stability or deepening of the junction scour. However, after flood 80, a large compound bar dominates the site and ongoing reworking (for example, by cross-bar channels) leads to a progressive change in deposits over time, producing a decrease in set thickness. Conversely, downstream of the confluence site where flow is confined to a single deep channel, reworking of the sediment towards the left bank due to thalweg migration, results in the deposits being 'reset' (Fig. 14B), such that although the deposits are eroded, they are replaced by packages of similar style and scale. As a result, the time series of median set thickness shows much less variability (for example, compare Fig. 14A and B).

## DISCUSSION

The results presented herein demonstrate that application of numerical modelling can provide

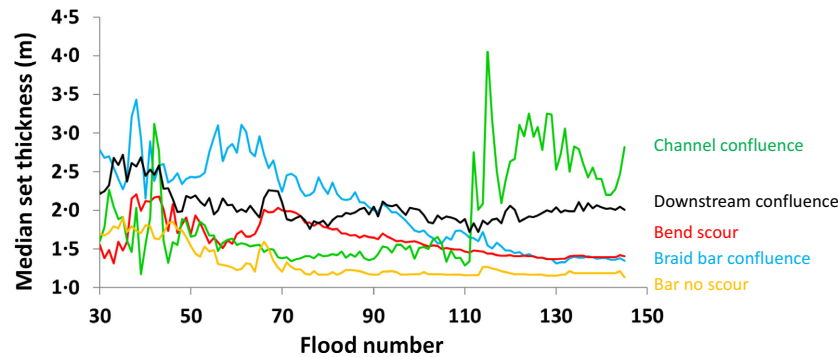


**Fig. 13.** Time series of median set thickness for the different scour zones discussed herein. Note how set thickness varies as accommodation space is created. For example, the channel confluence generates larger sets near the start of the simulation that then become truncated. However, as the scour migrates back, it generates new accommodation space that is then filled by larger sets. This behaviour contrasts with the braid bar confluence that is never reoccupied by scour, thus resulting in a gradual decline in set thickness over time.

unprecedented morphodynamic detail and insight into the sedimentological kinematics controlling alluvial scours. The model results highlight the diversity of scour types and that their fill has very different characteristics to non-scour settings. For example, the fill of bar-scale confluence scours is very similar to the model proposed by Bridge (2003) and Bridge & Lunt (2006) and is dominated by compound bar deposits, with about nine sets that become thinner towards the top of the fill due to repeated reworking. This style of scour fill also characterizes the outer bend scour, although more sets may be present in the vertical succession at these sites due to the greater depth of erosion. The main junction confluence scour has the potential to generate the thickest sets and can record evidence of single, thick, tributary mouth-bar sets, as suggested by Bristow *et al.* (1993) and Ullah *et al.* (2015) in the initial stages of fill. However, while set thickness may be greatest at such sites, the deposits of channel confluences may be reworked, so that single sets will not dominate the fill, and average set thickness will be an order of magnitude less than channel depth. From the perspective of the rock record, where limited exposure may preclude the measurement of a large number of unit bar sets, it is often more pragmatic to record the maximum set thickness. Since the section-averaged bankfull channel depths in the model are typically *ca* 10 m, an important point resulting from the simulations presented herein is that the maximum unit bar set thickness is approximately equivalent to the mean bankfull channel depth and not the scour depth (for example,

setH<sub>90</sub> at the bar and channel confluence was 7.1 m and 9.2 m, respectively). To place this in context, mean active unit bar height is *ca* 10 m, and thus mean bankfull channel depth is equivalent to mean unit bar height, which is equivalent to the maximum likely preserved set thickness. Thalweg depths are typically closer to 30 m at a section with maximum scour depths of 48 m. The migratory nature of the channel confluence scour, driven by shifts in the locations of the tributary channels, also results in these sites recording channel-scale successions of erosion surfaces, as suggested by Siegenthaler & Huggenberger (1993). The deep thalweg scour downstream of the confluence zone can also record the presence of thick sets, despite repeated episodes of reworking, because the flow is confined to a single channel and any eroded sediments are replaced by deposits of similar scale. This may result in a profile similar to that suggested by Ullah *et al.* (2015), although generated in a different way.

Thus, while results from the numerical model are entirely consistent with previous observations of confluence fill, they also reveal a much greater complexity, and highlight the importance of the nature of reworking that is not currently incorporated within any of the existing conceptual models. For example, the time series of basal scour behaviour (i.e. basal elevation change through time) is only one aspect of what determines preservation, in that the mobility of scours and bars and its role in determining the nature of erosion or deposition at a site must also be considered (for example, as illustrated in Figs 13 and 14). If a channel is in a relatively stable location, so that scour is spatially

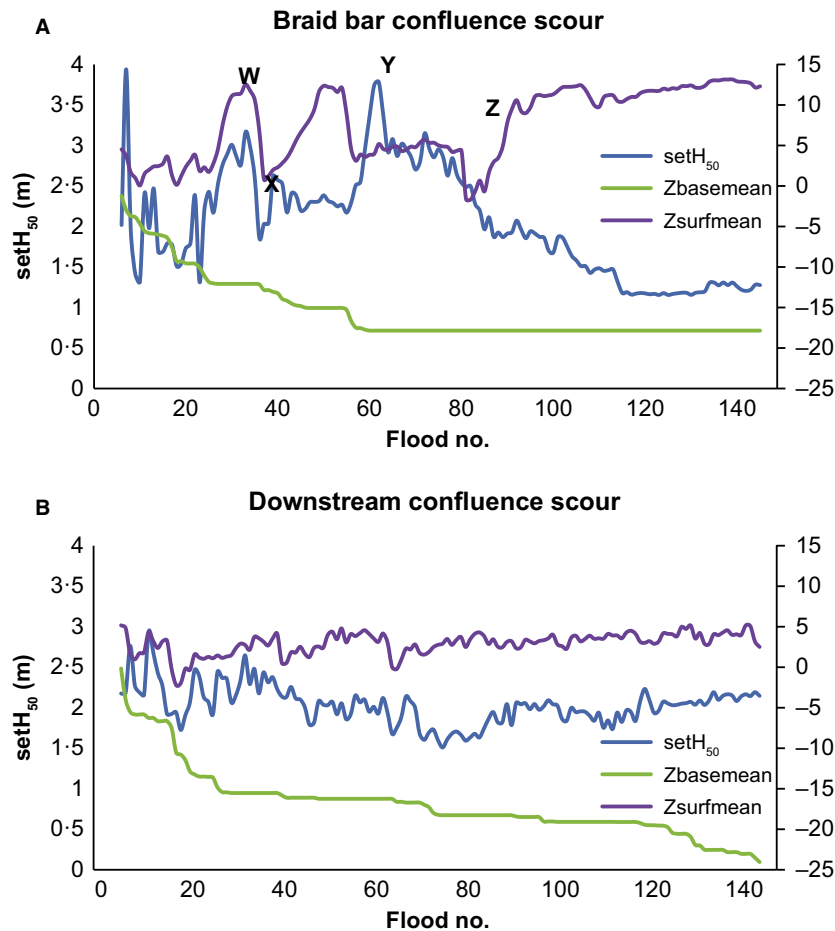


**Fig. 14.** Time series of median set thickness ( $setH_{50}$ ), mean surface elevation ( $Z_{surfmean}$ ) and mean basal scour elevation ( $Z_{basemean}$ ) for two contrasting scour types. (A) The active development of a braided system results in a complex time series of  $setH_{50}$ . As a bar moves into a previous channel  $setH_{50}$  increases (W), but then as a channel cuts across the site,  $setH_{50}$  subsequently decreases (X). The confluence reforms again prior to flood 60, creating accommodation space that is filled by a subsequent bar, resulting in a spike in  $setH_{50}$  (Y). From flood 80 onwards, a large compound bar dominates this location (Z) and hence new accommodation space is not created, the original sets are truncated by reworking related to cross-bar channels, and  $setH_{50}$  gradually decreases from flood 80 to the end of the simulation. (B) In contrast to Fig. 14A, this site has one deep channel that migrates from a central location towards the left bank. Thus, as some deposits are eroded, they become replaced with others of similar dimension. This is represented by the much less variable pattern in the topography and  $setH_{50}$ . From about flood 70 onwards, accommodation space increases slightly ( $Z_{basemean}$  decreases) that results in a slight increase in  $setH_{50}$ .

restricted, then the large sets that may be deposited initially become reworked and truncated. Conversely, if a scour site is mobile, the deposits may be largely 'reset' over time, such that the scour removes deposits but at the same time provides the space for new large-scale sets to replace them. Thus, there is no overall decline in set thickness over time and deposit characteristics remain largely constant. Such observations concur with recent work on dune preservation by Reesink *et al.* (2015), who highlight how the concept of a single preservation ratio is perhaps

too simplistic, and that preservation can be spatially highly heterogeneous and dominated by either erosion, deposition or variability in the time series of elevation. Such an interpretation thus suggests a strong link between scour morphodynamics and the resultant preserved deposits.

A key question that follows from these observations is what controls the morphodynamics of the main junction confluence scour itself? Based on the model simulations detailed herein, the behaviour of the scour appears to be related



principally to the characteristics of the tributaries upstream of the confluence. Thus, changes in channel configuration in the tributaries may lead to changes in the confluence (Figs 2, 3, 5 and 6). For example, increased sinuosity in the smaller tributary channel generates increased sinuosity of the downstream thalweg, which results in a scour that migrates downstream in a manner similar to a meander bend (Fig. 3). Likewise, as the incoming tributaries change the location of their convergence, this can result in a shift in the location of the main scour zone. For example, the current simulations show that flow in the smaller confluent tributary can alternate between the left and right side of the channel (Fig. 3), as also noted in the Ganges–Jamuna field site. Flow of the Ganges River originally joined much further to the north (Fig. 2), but as the channel has moved to the south, the main confluence scour has also migrated downstream.

The observations presented here have broader significance in two respects. Firstly, these results may explain the apparent difficulty in distinguishing ‘big rivers’ in the rock record (see Fielding, 2008; Miall, 2014). If large scours from large river confluences are preferentially preserved in the rock record, the high level of truncation of sets and erosional surfaces within their deposits may thus leave behind very little structure of a scale indicating that the deposits were associated with a large river [for example, median set thickness herein is *ca* 3 m (Table 1, Fig. 9) in a scour up to 48 m deep]. Even if the upper part of the succession is eroded, such as by channel abandonment and reoccupation following avulsion, preservation of just the largest sets at the base of the deposit will be equivalent in scale to the incoming channels (i.e. *ca* 10 m maximum) and not the full scour depth. Furthermore, the low angle of the large depositional and erosional surfaces recorded in the model and seismic data would suggest that only spatially extensive exposures would allow the correct identification and characterization of these features in the geological record. Secondly, such sediment reworking also makes differentiating between intrinsic autocyclic scour from a large river and allocyclic incised valley fill more problematic (see Fielding, 2008). Mapping of channel depth in order to permit confluence and bend scours to be placed within their correct context is rare in the geological record [see Ardies *et al.*, (2002) for a notable exception]. The results detailed herein suggest that since the scale of sets preserved in the scour will be much smaller

than the scale of the scour itself (Fig. 9), then this could potentially lead to erroneous interpretations of an incised valley fill. It is also worthy of note that the spatial extent of the channel-scale confluence scour will greatly exceed that of scours associated with bar-scale processes.

## CONCLUSION

This study provides a first demonstration of the potential for using a high-resolution numerical model to reconstruct the relationships between channel morphodynamics and the sedimentary deposits of large river confluences. While the model results presented herein are consistent with previous observations of the fill of confluence scours, the model output indicates a much higher degree of complexity in the morphodynamics, and heterogeneity of the resultant sedimentology, of these important fluvial sites. These results indicate that none of the existing conceptual models of confluence sedimentology can be applied easily, perhaps explaining why confluence scours are rarely reported in the literature. In addition, these results demonstrate that sediment reworking introduces further complexity into the identification of channel-scale versus valley-scale deposits. While the basal erosive surfaces produced by channel confluence scours may be large and extensive, the associated sedimentary fill is often significantly reworked, resulting in the preservation of sets that are of a similar order of magnitude to bar-scale confluence scours. There is thus an apparent mismatch between the scale of the erosional surfaces and that of the overlying depositional sets, which could lead to erroneous interpretations of valley-scale deposits. Most importantly, the present results highlight that an appreciation of the mobility of confluence zones must be taken into account to interpret correctly their deposits, a variable absent from current conceptual models. Given the high preservation potential of deep scours, the results presented herein provide important new concepts with which to interpret the rock record. Future modelling and field observations from other confluences, and other sites of appreciable scour, will allow additional testing of these ideas.

## ACKNOWLEDGEMENTS

This work was funded by a UK Natural Environment Research Council award to Sambrook

Smith (NE/I023228/1), Bull (NE/I023864/1) and Nicholas (NE/I023120/1). We are grateful to John Davis and Melis Cevatoglu for their support of seismic data acquisition. We thank Zahidul Islam Babu and the crew of the MV Kokilmoni for their assistance with the river surveys. Calculations for this study were performed using the University of Exeter Supercomputer. We thank the Associate Editor Charlie Bristow, Erik Mosselman and Janok Bhattacharya who helped to improve the clarity of the manuscript.

## REFERENCES

- Ardies, G.W., Dalrymple, R.W. and Zaitlin, B.A. (2002) Controls on the geometry of incised valleys in the basal quartz unit (lower Cretaceous), western Canada sedimentary basin. *J. Sediment. Res.*, **72**, 602–618.
- Best, J.L. and Ashworth, P.J. (1997) Scour in large braided rivers and the recognition of sequence stratigraphic boundaries. *Nature*, **387**, 275–277.
- Best, J.L. and Rhoads, B.L. (2008) Sediment transport, bed morphology and the sedimentology of river channel confluences. In: *River Confluences, Tributaries and the Fluvial Network* (Eds S.P. Rice, A.G. Roy and B.L. Rhoads), pp. 45–72. John Wiley & Sons, Ltd, Chichester. <https://doi.org/10.1002/9780470760383.ch4>.
- Bridge, J.S. (2003) *River and Floodplains: Forms, Processes and Sedimentary Record*. Blackwell, Oxford, 491 pp.
- Bridge, J.S. and Lunt, I.A. (2006) Depositional models of Braided Rivers. In: *Braided Rivers: Process, Deposits, Ecology and Management* (Eds G.H. Sambrook Smith, J.L. Best, C.S. Bristow and G.E. Petts), pp. 11–50. Blackwell Publishing Ltd, Oxford.
- Bristow, C.S., Best, J.L. and Roy, A.G. (1993) Morphology and facies models of channel confluences. In: *Alluvial Sedimentation* (Eds J. Puigdefabregas Tomas), Special Publications of the International Association of Sedimentologists, **17**, 91–100.
- Dixon, S.J., Sambrook Smith, G.H., Best, J.L., Nicholas, A.P., Bull, J.M., Vardy, M.E., Sarker, M.H. and Goodbred, S.L. (2018) The planform mobility of river channel confluences: insights from analysis of remotely sensed imagery. *Earth-Sci. Rev.*, **176**, 1–18.
- Fielding, C.R. (2008) Sedimentology and stratigraphy of large river deposits: recognition in the ancient record, and distinction from “incised valley fills”. In: *Large Rivers: Geomorphology and Management* (Ed. A. Gupta), pp. 97–113. John Wiley & Sons, Chichester.
- Gardner, J.T. and Ashmore, P.E. (2011) Geometry and grain-size characteristics of the basal surface of a braided river deposit. *Geology*, **39**, 247–250.
- Goodbred, S.L., Paolo, P.M., Ullah, M.S., Pate, R.D., Khan, S.R., Kuehl, S.A., Singh, S.K. and Rahaman, W. (2014) Piecing together the Ganges-Brahmaputra-Meghna River delta: Use of sediment provenance to reconstruct the history and interaction of multiple fluvial systems during Holocene delta evolution. *Geol. Soc. Am. Bull.*, **126**, 1495–1510. <https://doi.org/10.1130/B30965.1>.
- Huber, E. and Huggenberger, P. (2015) Morphological perspective on the sedimentary characteristics of a coarse, braided reach: Tagliamento River (NE Italy). *Geomorphology*, **248**, 111–124.
- van de Lageweg, W.I., van Dijk, W.M., Box, D. and Kleinhans, M.G. (2016) Archimetrics: a quantitative tool to predict three-dimensional meander belt sandbody heterogeneity. *Deposit. Rec.*, **2**, 22–46.
- Miall, A.D. (1985) Architectural-element analysis: a new method of facies analysis applied to fluvial deposits. *Earth Sci. Rev.*, **22**, 261–308.
- Miall, A.D. (2014) Updating uniformitarianism: stratigraphy as just a set of ‘frozen accidents’. In: *Strata and Time: Probing the Gaps in Our Understanding* (Eds D.G. Smith, R.J. Bailey, P.M. Burgess and A.J. Fraser), Geological Society, London, Special Publications, **404**, 11–36. <https://doi.org/10.1144/sp404.4>
- Nicholas, A.P. (2013) Morphodynamic diversity of the world’s largest rivers. *Geology*, **41**, 475–478.
- Nicholas, A.P., Ashworth, P.J., Sambrook Smith, G.H. and Sandbach, S.D. (2013) Numerical simulation of bar and island morphodynamics in anabranching megarivers. *J. Geophys. Res.*, **118**, 2019–2044.
- Paola, C. and Borgman, L. (1991) Reconstructing random topography from preserved stratification. *Sedimentology*, **38**, 553–565.
- Reesink, A.J.H., Ashworth, P.J., Sambrook Smith, G.H., Best, J.L., Parsons, D.R., Amsler, M.L., Hardy, R.J., Lane, S.N., Nicholas, A.P., Orfeo, O., Sandbach, S.D., Simpson, C.J. and Szupiany, R.N. (2014) Scales and causes of heterogeneity in bars in a large multi-channel river: Río Paraná, Argentina. *Sedimentology*, **61**, 1055–1085.
- Reesink, A.J.H., Van den Berg, J.H., Parsons, D.R., Amsler, M.L., Best, J.L., Hardy, R.J., Orfeo, O. and Szupiany, R.N. (2015) Extremes in dune preservation: controls on the completeness of fluvial deposits. *Earth Sci. Rev.*, **150**, 652–665.
- Sambrook Smith, G.H., Ashworth, P.J., Best, J.L., Woodward, J. and Simpson, C.J. (2005) The morphology and facies of sandy braided rivers: some considerations of spatial and temporal scale invariance. In: *Fluvial Sedimentology VII* (Eds M.D. Blum, S.B. Marriott and S.F. Leclair) IAS Special Publication, **35**, 145–158.
- Siegenthaler, C. and Huggenberger, P. (1993) Pleistocene Rhine gravel: deposits of a braided river system with dominant pool preservation. In: *Braided Rivers* (Eds J.L. Best and C.S. Bristow), Geological Society Special Publications, **75**, 147–162.
- Ullah, M.S., Bhattacharya, J.P. and Dupre, W.R. (2015) Confluence scours versus incised valleys: examples from the Cretaceous Ferron Notom Delta, southeastern Utah, USA. *J. Sediment. Res.*, **85**, 445–458.

Manuscript received 20 October 2017; revision accepted 5 June 2018